for an operator. However, while the eye has no problem distinguishing the rather distinctive appearance of particle tracks from background pits, accomplishing this reliably in software would be a formidable task.

In summary, this system provides a versatile, reasonably fast, and accurate means of making a measurement critical to evaluating ICF target performance.

ACKNOWLEDGMENT

This work was supported by the U. S. Department of Energy Office of Inertial Fusion under agreement No. DE-FC08-85DP40200 and by the Laser Fusion Feasibility Project at the Laboratory for Laser Energetics, which has the following sponsors: Empire State Electric Energy Research Corporation, New York State Energy Research and Development Authority, Ontario Hydro, and the University of Rochester. Such support does not imply endorsement of the content by any of the above parties.

1.C Neutron Diagnostics

Neutron diagnosis of compressed thermonuclear fuel has been an important gauge of target performance since the earliest days of laser-driven inertial confinement fusion. In this article, we will describe the neutron diagnostics used on a recent series of high-density target-implosion experiments to measure neutron yield, shell areal density, fuel areal density, and fuel ion temperature.

Our diagnostic philosophy during this campaign was to make simultaneous measurements of as many parameters as possible, using a variety of cross-checked techniques.

For deuterium-tritium (DT) fuel, we measure neutron yield using an activation technique based on the reaction $^{63}Cu(n,2n)^{62}Cu$. This activation results in decay by electron-positron annihilation, producing two 0.511-MeV gamma rays, which are detected in a standard slow coincidence system. The time intervals during which counting occurs are controlled automatically starting from laser irradiation time (Fig. 36.7). The advantages of the copper activation system include

1. high-energy threshold for the reaction (10.5 MeV) (reduces the effects of scattered neutrons),
2. relatively short half-life (manageable counting time and high decay rate),
3. the availability of a coincident reaction (reduces background), and
4. absolute-detector efficiency calibration using readily available nuclear sources.

In particular, the ability to measure the absolute detection system efficiency allows us to determine the thermonuclear yield of our

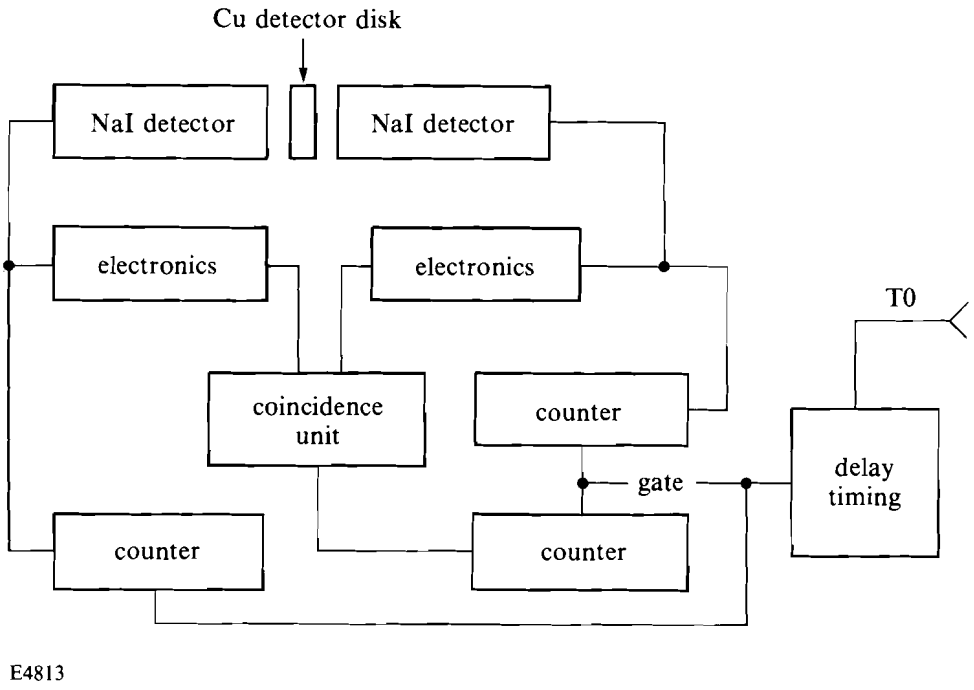

Fig. 36.7
Copper, slow-coincidence system. 'Electronics' consists of a photomultiplier tube preamplifier, amplifier, and timing single-channel analyzer. The detectors are enclosed in a 7.6-cm-thick lead jacket to shield from background radiation.

experiments from only geometric quantities and measured parameters. Thus,

$$Y = c\{\epsilon g\,[1 - e^{(-\sigma n l)}]\}^{-1} \quad ,$$

where Y is the neutron yield of the target; ϵ is the absolute detector efficiency; g is the solid angle subtended by the activation sample; σ is the cross section for the copper reaction; n is number density of copper atoms; l is the thickness of the copper activation sample; and c is the number of detected decays. The sensitivities and range of applicabilities of all our yield measurement systems are listed in Table 36.I.

Table 36.I
Detector positions, sensitivities, and sizes of yield measurement systems.

Detector	Solid Angle (% 4π)	Yield for 30% Error
2 m	0.050	1×10^5
3.5 m	0.016	3×10^5
4 m	0.003	1×10^6
LARD	0.250	1.5×10^4
Copper	0.005	7.8×10^6

E4546

Our second activation detector is a thermalizing detector employing the silver reactions:

$$^{107}\mathrm{Ag}(n, \beta^-)^{108}\mathrm{Ag}$$

and

$$^{109}\mathrm{Ag}(n, \beta^-)^{110}\mathrm{Ag} \ .$$

This device employs a neutron-thermalizing jacket of polyethylene surrounding four Geiger-Muller tubes wrapped with silver foil (Fig. 36.8). The cross sections for these reactions are a strong function of incident neutron energy. This, along with the fact that the neutrons incident on the detector system may be only partially thermalized by the polyethylene jacket, makes first-principle calibration of this detector difficult. Additionally, all thermalizing detectors are susceptible to scattering from diagnostics, experimental chamber, and support structures. However, the method is equally applicable for the measurement of DT or DD fuel primary yield and is our primary-yield diagnostic for pure DD fuel targets. We calibrate the silver detection system *in situ* against the copper activation system for DT fuel. For DD fuel, we calibrate the silver system by counting proton tracks in CR-39 track detector from the reaction branch:

$$^2\mathrm{D} + {}^2\mathrm{D} \rightarrow {}^3\mathrm{T} + p$$

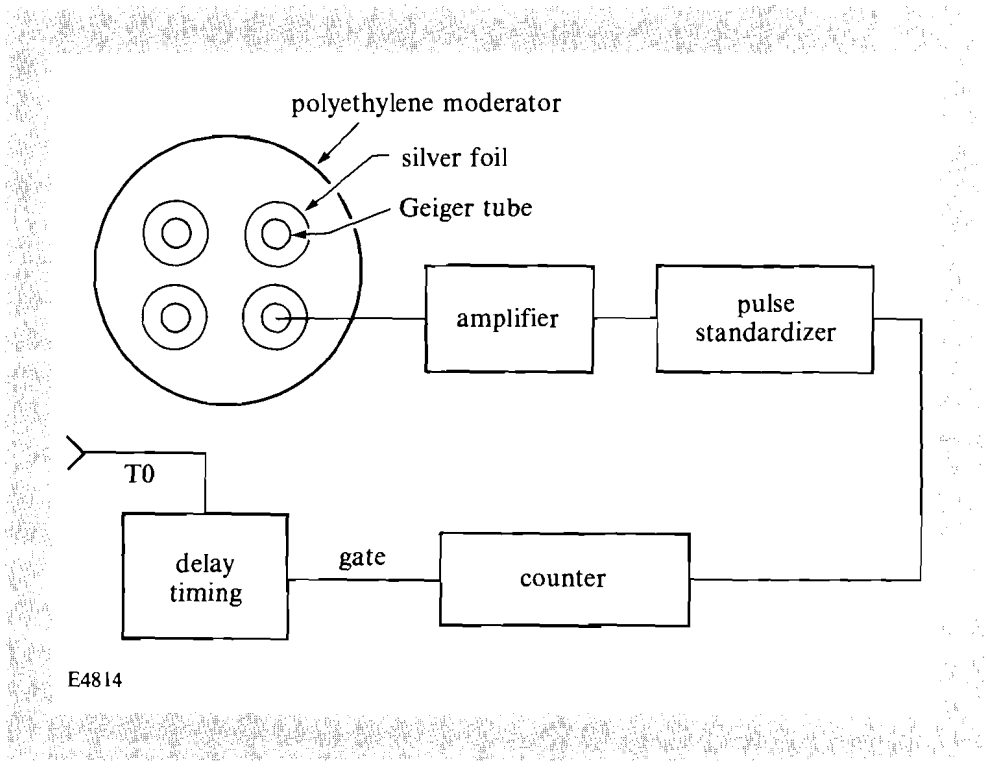

Fig. 36.8
Silver activation detector. The thermalizing jacket of polyethylene is 20 cm in diameter and 30 cm in length.

The number of tracks, along with the known track-detector geometry, measures the absolute yield from this reaction branch, which can be compared to the number of detected decays from the silver activation system to give the detector efficiency. Low-density, high-yield targets are used for these calibrations to reduce the slowing and stopping of 3.02-MeV protons in target and shell material.

A recent addition to the yield-measurement instruments utilizes a large (15-cm-diameter × 15-cm-length) sodium iodide activation detector. The sodium atoms in the detector are activated and "self-detected." This method utilizes the reaction:

$$^{23}\mathrm{Na}(n,\alpha)\ ^{20}F$$

$$^{20}F \rightarrow {}^{20}\mathrm{Ne} + \gamma(1.63\ \mathrm{MeV}) + \beta^{-}\ (5.4\ \mathrm{MeV})\ ,$$

which has a 4-MeV reaction threshold and an 11.4-s half-life. The detectors' large size, proximity to the target (85 cm), and short-activation half-life affords high sensitivity, low background, and simplicity of operation.

The activation-yield measurement systems described above have been integrated into the OMEGA shot summary reporting by using a CAMAC counter interfaced to the DEC PDP-11-based data acquisition system (Fig. 36.9). An IBM-PCAT-type microcomputer is used as a monitor to determine long- and short-term backgrounds and background histories. The microcomputer enables us to maintain an accurate assessment of the adjustment of the activation-detection systems.

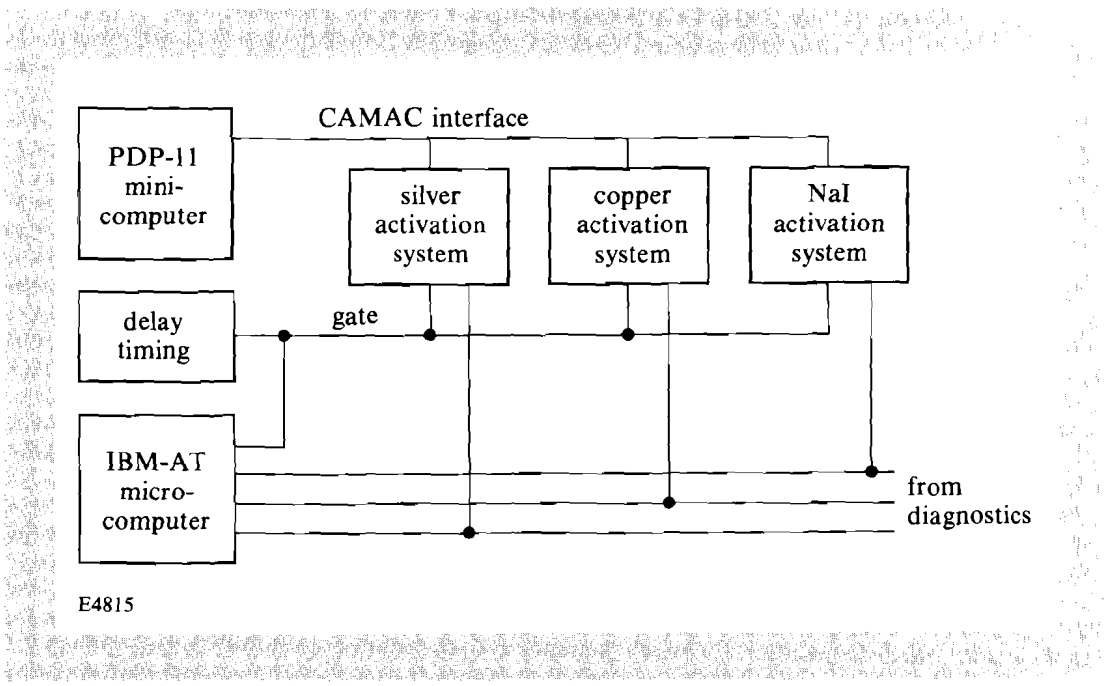

Fig. 36.9
Data collection and recording. The PDP-11 experimental operations minicomputer (CER) collects data from the experiment and generates a data base and a post-shot-data summary sheet. The IBM PC-AT-type microcomputer is equipped with five high-speed counters, recording pulses from the detection systems during background acquisition.

Neutron-averaged shell areal density $<\rho\Delta r>$ is measured using neutron activation of the silicon in the target shells. This technique, employing a highly efficient (35%) beta-gamma coincidence detector and a rapid-extraction, target-debris-collection system, has been described in several recent articles.[1,2] By using special low-activity shielding and carefully adjusting coincidence timing using a time-to-pulse height converter (TPHC), we have been able to reduce the background of this system to 0.3 counts per minute, extending the useful detection threshold to

$$Y < \rho \Delta r > \geq 1.3 \times 10^9 \frac{\text{mg}}{\text{cm}^2} .$$

The IBM-PCAT-type microcomputer mentioned above is also used to record the background history of the shell-density apparatus and monitor the decay rate of activated shell debris during data acquisition (Fig. 36.10).

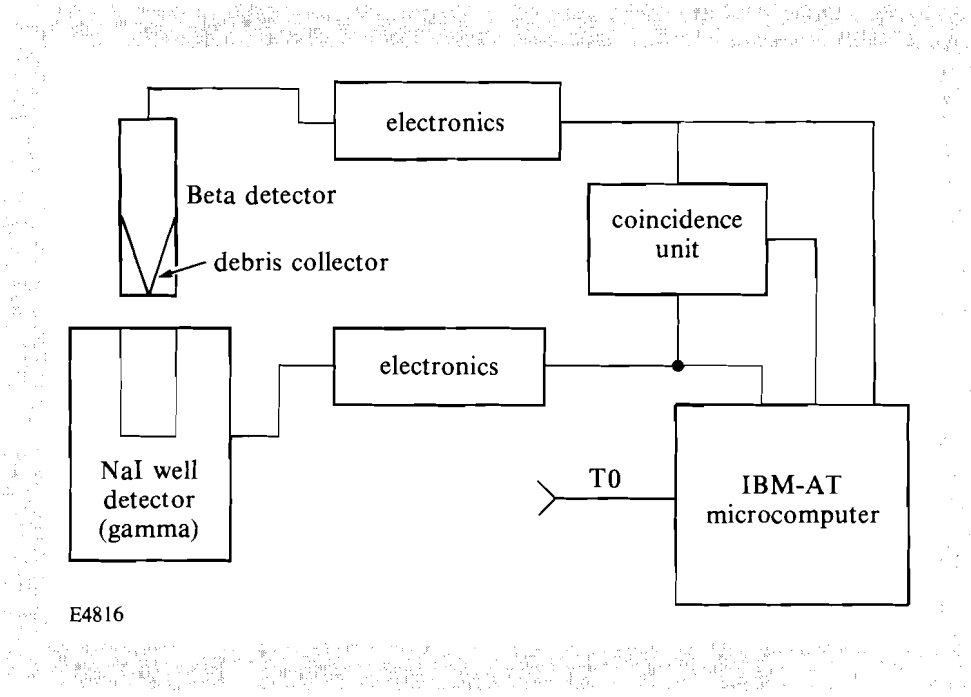

Fig. 36.10
Rad-chem system. The debris collection cone is placed in the beta detector after post-shot rapid extraction from the target chamber. The detectors form a beta-gamma coincidence system. 'Electronics' consists of a photomultiplier tube preamplifier, amplifier, and timing single-channel analyzer. The detectors are housed in 10 cm of low-activity lead, and 0.5 cm of copper to reduce background radiation.

Measurement of the yield of secondary DT fusion neutrons during the implosion of initially pure DD fuel targets has been suggested as a gauge of the fuel areal density.[3-6] Secondary neutrons result from the following reaction chains:

$$^2\text{D} + {}^2\text{D} \rightarrow n \text{ (2.45 MeV) ("primary" neutron)} + {}^3\text{He}$$

$$^2\text{D} + {}^2\text{D} \rightarrow {}^3\text{T} + p$$

$$^2\text{D} + {}^3\text{T} \rightarrow n \text{ (14.01 MeV) ("secondary" neutron)} + {}^4\text{He} .$$

The number of secondary neutrons produced in this reaction depends in a detailed way on the reaction cross sections, fuel density distribution, fuel temperature, and number density. For the simplest case of low-areal-density (< 10 mg/cm^2), high-temperature (10-KeV or more) fuel, it can be shown[4]:

$$< \rho r > = 12.05 \, N_{\text{DT}}/N_{\text{DD}} \text{ g/cm}^2 ,$$

where N_{DT} is the number of secondary neutrons and N_{DD} is the number of primary neutrons. For our target experiments, simulation of secondary/primary neutron ratio is obtained using a post-process job on the one-dimensional computer code *LILAC*.

The secondary measurement system employed during the recent campaign consists of four, large scintillator-photomultiplier assemblies. The detector packages are positioned at 2 m, 3 m, and 3.5 m from the target and provide a useful detection range of almost five orders of magnitude. Each detector is shielded from *n*-gamma scattering radiation by 1.5 cm of lead and is positioned so that the *n*-gamma pulse from the DD primary neutron burst is separated in time from the DT neutron signal by greater than the detector time resolution. This is important for unambiguous identification of detected signals. The smaller detectors (20-cm diameter, 10-cm thick) use Amperex type XP2020 photomultipliers coupled to plastic scintillators in light-tight aluminum housings, while the larger detectors (60-cm diameter, 15-cm thick) use RCA/Burle Industries type-8575 PMT's and liquid scintillator contained in a liquid-tight, reflective-paint-coated housing.

In the hydrogenous scintillating media that are used in our system, detection of neutrons is effected through elastic scattering of scintillator protons by the incident neutrons. The distribution of recoil proton energies depends on the differential scattering cross section as a function of angle. For the case of *n-p* scattering, the scattering is isotropic, giving a box spectrum extending from zero to the maximum neutron energy. Because of the distribution in proton recoil energies, there is not a one-to-one correspondence between observed photomultiplier charge and neutron flux. This results in poorer statistics than would be expected from a conventional pulse-counting system. In the limit of large numbers of detected neutrons or large (total capture, thermalizing) detectors the statistical error associated with this process is small. Our strategy has been to maximize the solid angle and detection efficiency of the scintillator system to reduce this statistical error.[7]

The scintillator system is calibrated on pure DT fuel shots by comparison with the copper activation system. In order to avoid saturating the photomultipliers, calibration shots are done with reduced photomultiplier gain and/or optical filters in front of the photomultipliers. The scintillating medium itself is linear over many decades of light output. This calibration gives the average detected charge per neutron, but does not measure the distribution of detected charge. The width of the current-pulse distribution associated with the recoil protons is measured by irradiating each detector with neutrons from a californium-252 spontaneous fission source and measuring the current-pulse-height distribution using a conventional nuclear counting system. Since the californium source has a broad neutron energy distribution, the width of the current pulse distribution is greater than that obtained with a monoenergetic neutron source. Both the linearity and gain of the each photomultiplier are measured with a pulsed light source.

The fuel-ion temperature for these experiments was measured by time-of-flight neutron spectroscopy. This method, as applied to inertial confinement fusion, was originally described by Brysk.[8] Two detectors are deployed, at 1.8 m and 10 m, for DD and DT neutrons, respectively. These spectrometers consist of a quenched scintillator

(Bicron BC-422, 1% quench) optically coupled to a channel-plate photomultiplier (ITT f4129). The photomultipliers are installed in housings designed to eliminate electrical discontinuities and pulse distortion (Fig. 36.11). The nearly Gaussian output pulse from this detector is shown in Fig. 36.12. The recording system, alignment, and collimation of this detector have been described previously.[1] For the present detector distances and system time resolution, the minimum measurable ion temperatures are

DT fuel (14-MeV neutrons): $T = 0.8$ KeV for $Y > 3 \times 10^8$,

DD fuel (2.45-MeV neutrons): $T = 0.8$ KeV for $Y > 10^7$.

The data from the experiment, consisting of oscillographic recordings on film, is hand digitized and fit to a Gaussian waveform to give the fuel-ion temperature.

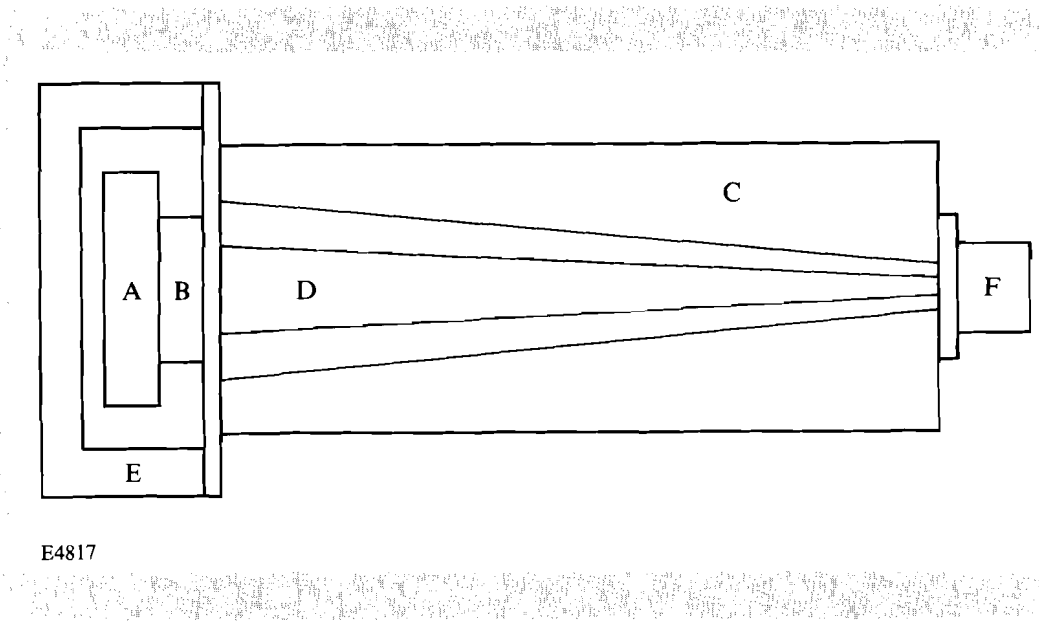

Fig. 36.11
Neutron time-of-flight detector (cross section). (A) scintillator, BC-422; (B) ITT f4129 PMT; (C) outer housing; (D) inner coaxial line; (E) lead x-ray shielding; (F) output connector.

In summary, we have employed a number of cross-checked detectors on recent experiments to measure neutron yield, shell areal density, fuel areal density, and fuel-ion temperature. Where possible, multiple detectors are used to measure important parameters, such as primary neutron yield.

ACKNOWLEDGMENT

This work was supported by the U. S. Department of Energy Office of Inertial Fusion under agreement No. DE-FC08-85DP40200 and by the Laser Fusion Feasibility Project at the Laboratory for Laser Energetics, which has the following sponsors: Empire State Electric Energy Research Corporation, New York State Energy Research and Development Authority, Ontario Hydro, and the University of Rochester. Such support does not imply endorsement of the content by any of the above parties.

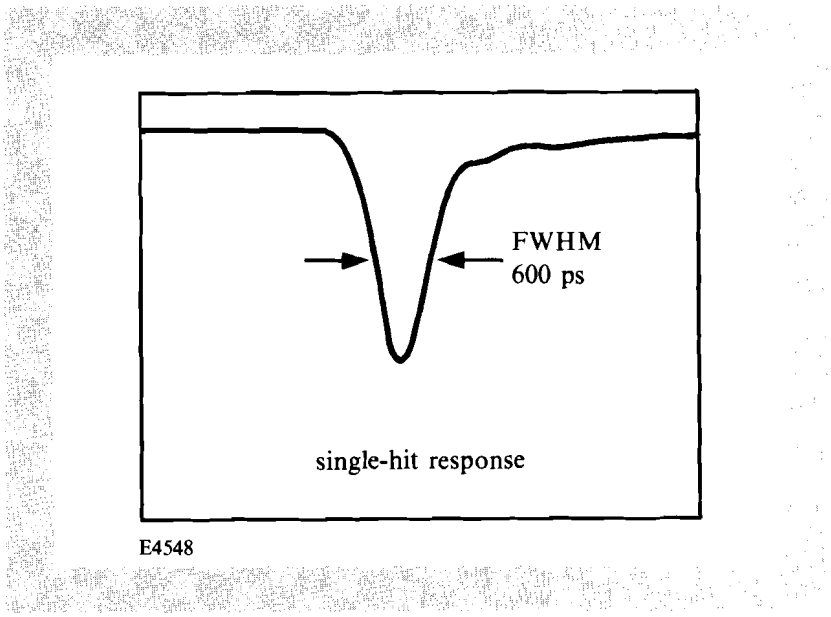

Fig. 36.12
Neutron time-of-flight detector output pulse.

REFERENCES

1. LLE Review **27**, 103 (1986).
2. S. M. Lane, E. M. Campbell, and C. Bennett, *Appl. Phys. Lett.* **37**, 600 (1980).
3. E. G. Gamalii *et al.*, *JETP Lett.* **21**, 70 (1975).
4. T. E. Blue and D. B. Harris, *Nuc. Sci. Eng.* **77**, 463 (1981).
5. M. D. Cable and S. P. Hatchett, *J. Appl. Phys.* **62**, 2233 (1987).
6. H. Azechi *et al.*, *Appl. Phys. Lett.* **49**, 555 (1986).
7. *Radiation Detection and Measurement*, edited by G. F. Knoll (Wiley and Sons, NY, 1979), pp. 576-584.
8. H. Brysk, *Plasma Phys.* **15**, 611 (1973).